

Tsutsumi YM, Tsutsumi R, Hirokawa YT, Sakai Y, Hamaguchi E, Ishikawa Y , Yokoyama U, Kasai A, Kambe N, and Tanaka K.	Geranylgeranylacetone protects the heart via caveolae and caveolin-3.	Life Sciences.	101,	43-48	2014
Okumura S, Fujita T, Cai W, Jin M, Namekata I, Mototani Y, Jin HL, Ohnuki Y, Tsutsuneoka Y, Kurotani R, Suita Km Kawakami Y, Hamaguchi S, Abe T, Kiyonari H, Tsunematsu T, Bai Y, Suzuki S, Hidaka Y, Umemura M, Ichikawa Y, Yokoyama U, Sato M, Ishikawa F, Izumi-Nakaseko H, Adachi-Akane S, Tanaka H, and Ishikawa Y .	Disruption of Epac1 decreases phosphorylation of phospholamban and protects the heart against stresses.	J. Clin. Invest.		in press	2014
Baljinnyam E, Umemura M, Chuang C, De Lorenzo M, Iwatsubo M, Chen S, Goydos J, Ishikawa Y , Whitelock J, and Iwatsubo K.	Epac1 increases migration of endothelial cells and melanoma cells via FGF2-mediated paracrine signaling.	Pigment Cell & Melanoma Research.		doi: 10.1111/pcmr.12250. [Epub ahead of print]	2014 Apr 11.
Yokoyama U, Iwatsubo K, Umemura S, Fujita T, and Ishikawa Y .	The prostanoid EP4 receptor and its signaling pathway.	Pharmacol Rev.	65,3	1010-1052	2013
Okamoto Y, Hirota M, Monden Y, Murata S, Koyama C, Mitsudo K, Iwai T, Ishikawa Y , and Tohnai I.	High-dose zoledronic acid narrows the periodontal space in rats.	Int J Oral Maxillofac Surg.	42,5	627-631	2013

Lai L , Yan L, Gao S, Hu CL, Hui G, Davidow A, Park M, Bravo C, Iwatsubo K, Ishikawa Y, Auwerx, J, Sinclair D, Vatner SF, and Vatner DE.	Type Type 5 Adenylyl Cyclase Increased Oxidative Stress by Transcriptional Regulation of MnSOD via the Sirt1/FoxO3a Pathway.	Circulation.	127,16	1692-1701	2013
Eijkelkamp N, Linley JE, Torres JM, Bee L, Dickenson AH, Gringhuis M, Minett MS, Hong GS, Lee E, Oh U, Ishikawa Y, Zwartkuis FJ , Cox JJ, and Wood, JN.	A role for Piezo2 in EPAC1-dependent mechanical allodynia.	Nature Commun.	4	1682	2013
Wang H, Heijnen CJ, van Velthoven CTJ, Willemen HLD, Ishikawa Y, Zhang X, Sood AK, Vroon A, Eijkelkamp N, and Kavelaars A.	Balancing GRK2/ Epac1 levels prevents and relieves chronic pain.	J. Clin. Invest.	123,12	5023-5034	2013
Vatner SF, Park M, Yan L, Lee G, Lai L, Iwatsubo K, Ishikawa Y, Pessin J, and Vatner DE.	Adenylyl cyclase type 5 in cardiac disease, metabolism and aging, Adenylyl Cyclase Type 5 in Cardiac Disease, Metabolism and Aging.	Am J Physiol Heart Circ Physiol.	305,1	H1-8	2013

Jeun M, Lee S, Kim JY, Jo YH, Park HK, Paek HS, Takemura Y, and Bae S.	Physical Parameters to Enhance AC Magnetically Induced Heating Power of Ferrite Nanoparticles for Hyperthermia in Nanomedicine.	IEEE Transactions on Nanotechnology.	Vol.12, Issue 3	314-322	2013
Ota S, Takahashi Y, Tomitaka A, Yamada T, Kamid D, Watanabe M, and Takemura Y.	Transfection efficiency influenced by aggregation of DNA/polyethyleneimine max/magnetic nanoparticle complexes.	Journal of Nanoparticle Research.	15,1653	1-12	2013
Nakamura K, Ueda K, Tomitaka A, Yamada T, and Takemura Y.	Self-heating temperature and ac hysteresis of magnetic iron oxide nanoparticles and their dependence on secondary particle size.	IEEE Transactions on Magnetics.	49	240-243	2013
Miyake Y, Kumagai K, Watabe K, Yamada T, Sato T, and Takemura Y.	Heat Control of Resonant Circuit for Hyperthermia Implant.	IEEE Transactions on Fundamentals and Materials.	133	362-365	2013
Hoshino Y, Oyaizu M, Koyanagi Y, and Honda K.	Enantiomerically Enriched Bicyclic Hydroxamic Acids in One Step from α -Aminohydroxamic Acids and keto Acids via Cyclocondensation.	Synthetic Communications.	43	2484-2492	2013
Hattori S, Hagihara S, Ohira K, Aoki I, Saga T, Suhara T, Higuchi M, and Miyakawa T.	In vivo evaluation of cellular activity in α CaMKII heterozygous knockout mice using manganese-enhanced magnetic resonance imaging (MEMRI).	Front Integrative Neurosci.	11;7:76.	PubMed PMID: 24273499; PubMed Central PMCID: PMC3822296	2013
Takanashi JI, Nitta N, Iwasaki N, Saito S, Tanaka R, Barkovich AJ, and Aoki I.	Neurochemistry in shiverer mouse depicted on MR spectroscopy.	J Magn Reson Imaging.	doi:10.1002/jmri.24306. [Epub ahead of print]	PubMed PMID:24243812.	2013

Mi P, Kokuryo D, Cabral H, Kumagai M, Nomoto T, Aoki I, Terada Y, Kishimura A, Nishiyama N, and Kataoka K.	Hydrothermally synthesized PEGylated calcium phosphate nanoparticles incorporating Gd-DTPA for contrast enhanced MRI diagnosis of solid tumors.	J Control Release.	doi:pII: S0168-3659(13)00887-0. 10.1016/j.jconrel.2013.10.038.[Epub ahead of print] PubMed PMID: 24211705.		2013
Murayama S, Joji, Shibata Y, Liang K, Santa T, Suga T, Aoki I, and Kato M.	A Simple Preparation of Polyethylene Glycol-Based Soft Nanoparticle Containing Dual Imaging Probes.	J Mater Chem B Mater Biol Med. 2013			in press, 2013
Takuwa H, Tajima Y, Kokuryo D, Matsuura T, Kawaguchi H, Masamoto K, Taniguchi J, Ikoma Y, Seki C, Aoki I, Tomita Y, Suzuki N, Kanno I, and Ito H.	Hemodynamic changes during neural deactivation in awake mice: A measurement by laser-Doppler flowmetry in crossed cerebellar diaschisis.	Brain Res.	doi:pII:S0006-8993(13)01297-3. 10.1016/j.brainres.2013.09.023. [Epub ahead of print] PubMed PMID: 24076448.		2013
Maruyama M, Shimada H, Suhara T, Shinotoh H, Ji B, Maeda J, Zhang MR, Trojanowski JQ, Lee VM, Ono M, Masamoto K, Takano H, Sahara N, Iwata N, Okamura N, Furumoto S, Kudo Y, Chang Q, Saido TC, Takashima A, Lewis J, Jang MK, Aoki I, Ito H, and Higuchi M.	Imaging of tau pathology in a tauopathy mouse model and in Alzheimer patients compared to normal controls.	Neuron.	79,6	1094-1108	2013
Zhelev Z, Bakalova R, Aoki I, Lazarova D, and Suga T.	Imaging of Superoxide Generation in the Dopaminergic Area of the Brain in Parkinson's Disease, Using Mito-TEMPO.	ACS Chem Neurosci.	[Epub ahead of print] PubMed PMID:24024751.		2013

Enomoto T, Kawano M, Fukuda H, Sawada W, Inoue T, Hara KC, Kita Y, Sakamoto S, Yamaguchi Y, Imai T, Hatakeyama M, Saito S, Sandhu A, Matsui M, Aoki I, and Handa H.	Viral protein-coating of magnetic Nanoparticles using simian virus 40 VP1.	J Biotechnol.	167,1	8-15	2013
Sawada K, Horiuchi-Hirose M, Saito S, and Aoki I.	MRI-based Morphometric Characterizations of sexual Dimorphism of the cerebrum of ferrets (<i>Mustela putorius</i>).	Neuroimage.	doi:pii: S1053-8119(13)00661-7. 10.1016/j.neuroimage.2013.06.024. [Epub ahead of print] PubMed PMID: 23770407.		2013
Saito S, Hasegawa S, Sekita A, Bakalova R, Furukawa T, Murase K, Saga T, and Aoki I.	Manganese-enhanced MRI reveals early-phase radiation-induced cell alterations in vivo.	Cancer Res.	73,11	3216-3224	2013
Kokuryo D, Anraku Y, Kishimura A, Tanaka S, Kanomura MR, Kershaw J, Nishiyama N, Saga T, Aoki I, and Kataoka K.	SPIO-PICsome: Development of a highly sensitive and stealth-capable MRI nano-agent for tumor detection using SPIO-loaded unilamellar polyion complex vesicles (PICsomes).	J Control Release.	doi:pii: S0168-3659(13)00159-4. 10.1016/j.jconrel.2013.03.016. PubMed PMID: 23542239.		2013
Bakalova R, Zhelev Z, Aoki I, and Saga T.	Tissue redox activity as a hallmark of carcinogenesis: from early to terminal stages of cancer.	Clin Cancer Res.	19,9	2503-2517	2013

Iida S, Imai K, Matsuda S, Itano O, Hatakeyama M, Sakamoto S, Kokuryo D, Okabayashi K, Endo T, Ishii Y, Hasegawa H, Aoki I, Handa H, and Kitagawa Y.	In vivo identification of sentinel lymph nodes Using MRI and size-controlled and monodispersed magnetite nanoparticles.	J Magn Reson Imaging.	doi:10.1002/jmri.24108. [Epub ahead of print] PubMed PMID: 23554026.		2013
Nikolova B, Kostadinova A, Dimitrov B, Zhelev Z, Bakalova R*, Aoki, I and Tsoneva I.	Fluorescent imaging for assessment of the molecular mechanisms of combined application of electroporation and rifampicin on HaCaT cells as a new therapeutic approach in psoriasis.	Sensors (Basel).	13,3	3625-3634	2013
Tanimoto E, Karasawan S, Ueki S, Nitta N, Aoki I, and Koga N.	Unexpectedly large water-proton relaxivity of TEMPO incorporated into micelle-Oligonucleotide.	RSC Adv.	3 DOI:10.1039/C3RA22372H. Accepted.	3531-3534	2013

雑誌

和文

発表者氏名	論文タイトル名	発表誌名	巻号	ページ	出版年
石川義弘 江口晴樹	切らずに治すがん治療薬の開発	化学工業	Vol.64, No.1	1-5	2013
石川義弘、 江口晴樹	磁性医薬品の開発—他業種の成熟技術の導入によるブレークスルー—	Pharm Tech Japan,	Vol.29	88-92	2013
石川義弘	未来医療への架け橋 がん治療 磁石の力応用試みる	神奈川新聞			2013.11.8
Eguchi Haruki Ishikawa Yoshihiro	IHI: Patent issued for drug, drug guidance system, magnetic detection system, and drug design method.	Biotech Week			2014,4.16
横山 詩子 石川義弘	大動脈瘤の進展とPGE ₂	遺伝子医学MOOK	24	296-300	2013
竹村泰司	特集：磁気を利用する体にやさしい治療 -磁気と医療のこれから-	電気学会誌	Vol.133	72-73	2013

[IV]

研究成果の刊行物・別刷

平成25年度第三次対がん総合戦略研究事業

研究課題： 悪性中皮腫に対する単剤多機能抗がん治療の開発

課題番号： H24-3次がん一般-005

研究代表者：横浜市立大学大学院医学研究科 循環制御医学

：石川義弘

1. 本年度の研究成果

石綿による健康被害（石綿症）は1900年代から知られていたが、我が国で法規制が開始されたのは75年以降であり、本格的な労働者に対する規制は2005年以降である。悪性中皮腫は胸膜中皮由来の腫瘍であり石綿暴露との関連が強いが、発症まで20-50年を要する。このため今後十数年間は我が国の患者数の増加が予測される。発見時には外科的根治術が困難であり、放射線や化学治療にも腫瘍としての抵抗性が強く、極めて低い治療成績である。化学療法としてシスプラチン、或はペメトレキセド併用療法が基本だが、薬剤の投与量は、副作用の発現によって制限を受ける。また一部の先進医療機関では、温熱療法が併用されているが、症状緩和に有効ではあるが、積極的な治療法ではない。

悪性腫瘍に対する温熱療法の歴史は19世紀と古いが、現代的な治療に応用されたのは60年代からである。細胞実験ではがん細胞は42.5度以上になると細胞死を起こしやすくなる。そこで電磁波を用いてがん組織全体を暖め、化学療法の効果の増強を狙ったマイルド温熱による全身温熱療法が採用されている。これはあくまでも化学療法の補助療法であり、副作用は少ないが治療効果も高度ではない。近年欧米で実用化された方法は、局所温熱による積極的な治療法である。鉄などの磁性微粒子を腫瘍組織に直接注入し、交流磁場印加によって発熱させ、がん細胞を殺傷する仕組みである。然るに使用されるのは抗がん作用を持たない鉄粒子を発熱体として使用するのみである。抗がん剤を腫瘍組織に同時注入すると、磁性粒子による発熱のため抗がん剤が変性してしまうからである。温熱治療と化学療法が同時施行できれば、治療効果は画期的に増強することが期待できる。

我々の研究では、これまで治療困難とされる悪性中皮腫に対して、化学療法と温熱療法の「同時施行」を検討した。このためには既存の抗がん剤や鉄粒子ではなく、新規磁性抗がん剤（E1236）を用いる。シスプラチン様の強い抗がん作用を有するだけでなく、交流磁場印加によって強い発熱作用を持つ。このため抗がん作用が熱変性することがなく、反復性の交流磁場印加・温熱治療が可能であることが分かった。中皮腫細胞が温熱感受性をもち、本抗がん剤を中皮腫局所に磁場誘導することができ、さらに交流磁場印加で発熱できれば、温熱・化学療法の同時施行ができるようになり、悪性中皮腫に対して有効性を高めた治療法として開発ができると考えられた。とりわけ欧米で先鞭をつけられた鉄微粒子による局所温熱療法に対して、それを凌駕する画期的ながん治療法を日本から世界に向けて発信することができると考えられる。

昨年度からの継続実験において、ヒト由来の悪性中皮腫細胞における温熱感受性を検討した。ヒト由来の細胞株は複数種確立されており、これらの異なった株種に対して同様の検討を行った。温熱感受性については株間でも類似し、42度で効果を示すが、43度程度にまで上昇させても温熱感受性を示すことが分かった。温熱感受性は狭い温度域でのみ有効なわけではなく、他の癌細胞腫と同様に比較的ひろい温度枠を設定することができることが分かった。またこの温度枠において、EI236との併用によりいずれも抗がん活性が亢進することが確認された。昨年度の実験結果から、EI236が10 μ M前後において温熱刺激なしで50%程度の生存性が、温熱存在下においては最大30%以下に低下し、さらに薬剤濃度を高めると、細胞生存性は容量依存性に低下するが、温熱による細胞殺傷増強作用は低下することがわかっている。本年度の結果と合わせて、温熱効果が最大限に発揮できる抗がん剤濃度を検討し、最低量の治療濃度で治療を行うことが、効果的な治療法に結びつくことが確認された。

EI236の発熱特性の制御には、薬剤濃度以外に、交流磁場発生装置の性能が重要な役割を果たすことが分かった。これは出力だけの問題ではなく、使用する周波数と電力によって規定されることが分かった。さらに周波数特性によって、深部到達度を調節できることがわかり、これは悪性中皮腫の治療にあたって、皮膚からの深度により、周波数特性を変化させることによって発熱効果を最適化できることが分かった。我々の試作機であるYOKI-1500は単一条件でEI236に高い発熱を起こさせるが、さらに、周波数特性変換機能を持たせた機械によって、発熱や深部を調節できることがわかった。悪性中皮腫においても胸腔内での発現部位や深度が異なることから同機能は重要であると考えられた。

昨年度の研究結果から、マウス生体レベルで胸腔内において集積させることが可能であることがわかったが、これには大型棒磁石を体表面から当てるか、特殊小型磁石を胸腔皮下に埋め込むことが必要であった。然るに、ヒト応用にあたっては実用的ではない。そこでピックアップ盤様の小型磁石を衣料ベストに縫込み、動物に磁石入りベストを着用させることで胸腔部分への集積が可能であるかを検討した。市販の小型磁石を縫い込んだベストを作成し、EI236を胸腔内に注入した後に、磁石部分がマウス胸壁にあたるようにベストを装着させ、マウスを3日間自由行動とさせた。マウス胸壁を取り出し、EI236を特殊染色したところ、ベスト磁石装着部に一致して強い集積反応が見られた。このことは磁石ベスト装着によってEI236を局所に誘導できたことを示す。同様の実験を腹腔においても行ったところ、強い集積を得ることができた。ヒトにおいてはさらに強力な小型磁石が複数必要になると考えられるが、極めて低い侵襲性で、体表面から磁場誘導を胸壁に対してかけることが可能と考えられる。

EI236による治療効果の評価においては、動物モデルでは胸壁を摘出せねばならず、時間経過による治療効果を実験的に評価することが困難である。そこで生体レベルで中皮腫組織の増減を観察できるよう、MRIによる画像診断の手法を開発した。先行研究から、マウスに中皮腫を移植して、マウス悪性中皮腫モデルを作成することが可能であることが分か

っている。このモデルにおいて、MRIの撮影条件を検討することにより、中皮腫のMRIによる非侵襲的な形態観察が可能であることがわかった。さらに確立された悪性中皮腫マウスモデルにおいて、EI236を投与し、体表面から磁場誘導をかけた。このMRI画像モデルにおいても、EI236がMRIシグナルとして検出できることが分かった。このことは、悪性中皮腫患者にEI236を投与した場合に、薬剤が腫瘍部位にどの程度到達したかを判定する可能性を強く示すものである。さらに磁場誘導をかけた後に、腫瘍部位への集積の程度を非侵襲的に定量する可能性を示す。

さらに我々は、理研のSpring8を用いたEI236の結晶構造解析結果から、数十年前に開発され、現在世界で幅広く使用されている既存の抗がん剤を磁性化した。この磁性抗がん剤は、抗がん作用として基本的な薬理学的な特徴を維持しながら、磁場誘導によって局所に誘導させることが可能であることが分かった。さらにMRIにおいて画像測定が可能であることも分かった。

以上の平成25年度の実験結果から、1)多数のヒト悪性中皮腫細胞株はEI236に対して高い薬剤感受性と温熱感受性を示すこと、2)交流磁場印加装置の最適化により、組織における磁場印加の条件が検討され、この条件下でヒトへの応用性が高まること、3)マウス生体レベルで非侵襲的に磁石によるEI236の集積方法が確立されたこと、4)EI236の治療効果を経時的に観察できるマウス悪性中皮腫モデルが確立され、マウス生体において磁場誘導をMRIで評価することができること、5)既存の抗がん剤の磁性化ができること、が判明した。これらの検討結果は、EI236を用いた悪性中皮腫の新規治療法の開発が極めて有望なものになる可能性が示された。今後はさらにヒト臨床応用を目標に、研究を進展させていきたい。

2. 研究成果の意義および今後の発展性

抗がん剤に限らず一般の医薬品化合物は、磁場誘導に対して十分な磁性を持たないとされる。しかしコバルトや鉄（磁性）粒子は磁石に付く。そこで磁性鉄粒子を利用して温熱療法や磁場誘導を行う研究が60年代より進められてきた。一般的な手法は、鉄粒子と抗がん剤を混ぜ合わせてリポソームに包み、全体を磁石で誘導する。しかしながら、合成段階において抗がん剤と鉄粒子の両方が確実にリポソームに包埋されているのか、あるいは比率が1:1で常に包埋されるかなどの問題があった。さらには空リポソームの存在や、熱やpHによってリポソームが変性分解するため不安定、経口投与が困難などの諸問題がある。とくに温熱療法との併用においては、熱によってリポソームが分解してしまうため、施行が困難である。

造船業における船舶の金属材料の開発には磁性の制御が必須であり、IHI（株）の基盤技術研究所では高度な磁性評価の技術を有する。エレクトロニクス分野ではこの技術を有機ダイオードなどの開発に応用している。我々はそれを医薬品化合物に応用し、新規磁性抗がん剤化合物（EI236）が開発された。本抗がん剤はシスプラチン類似薬であり、IHI（株）

(旧石川島播磨重工業)の造船業におけるエンジンの金属材料開発技術を、医薬品化合物開発に応用して開発された。横浜市立大学先端医科学研究センターの援助を受けて実用化の検討段階に移行しており、多数の国内・国際特許によっても支持された独占的な先進技術である。本研究は学際的な共同研究者よりなる。本研究で対をなす温熱・磁場装置に関しては、横浜国大をはじめとする工学研究者（竹村泰司教授）との協力を得て試作品 YOKI-1500 による検討を繰り返してきた。本年度の研究成果から、本試作品をどのように改良していくかの道筋が示された。また放射医学総合研究所のMRI分子イメージ専門家（青木伊知男チームリーダー）による悪性中皮腫の検討においては、生体レベルで EI236 を可視化することに成功している。これは画像化可能な抗がん剤として重要な役割を果たすことができると考えられる。

過去8年間に及ぶ先行研究において、磁性を有する抗がん剤化合物が複数同定された。本年度の研究成果から、新規磁性抗がん剤を見つけるだけでなく、既存の抗がん剤に対して磁性特性を付与することが可能であることが示された。同様の手法を用いることにより、抗がん剤のみならず、他分野の医薬品化合物を磁性化する可能性が生まれた。これは患部への集積が望ましいと考えられる医薬品すべてに磁性化特性を与えることにより、磁場誘導により局所化できる可能性をしめす。さらに MRI による生体レベルでの画像化が可能であることから、生体内に投与した後どのような分布を示すのかを画像診断することが可能になると期待される。本技術は純国産技術であり、学際技術であるとともに、造船業の技術を医学に転用した、産学連携の象徴的な技術開発であると考えられ、今後の我が国の産業振興にも貢献できると考えている。

今後数十年間にわたって患者が増大すると考えられる悪性中皮腫の根治的治療法は胸膜肺全的術であるが、診断時にはすでに広範に進展していることが多く、外科手術の適応とならないことが多い。外科治療は侵襲的であり、死亡率は高齢者ほど高いため、好発する高齢者でむしろ慎重な対応が必要である（日本肺癌学会ガイドライン）。手術不適応例に対しては放射線療法や化学療法がおこなわれるが、抗がん剤による治療は75歳以上の高齢者には推奨されていない。そのため今後増加が予測されている高齢者に対する化学療法としては、国民的な解決課題と考えられる。高齢者は抗がん剤に対して副作用の発現が高いため、少量で有効な抗がん剤が必要である。また肝腎機能の低下により、副作用の発現予想が困難である。そこで体表面積から類推するだけでなく、テーラーメイド的な投与量の決定が必要である。さらに症状緩和だけを目的とした温熱療法ではなく、治療効果の増強が期待できるハイパーサーミア療法の確立が必要である。磁性抗がん剤はそのいずれにも対応できる抗がん治療が可能であり、とりわけ「胸膜は胸壁から浅い」ため、磁場による誘導（ドラッグデリバリー）が可能となり、磁性抗がん剤の適応である。今回の検討結果から、その実用化への可能性が強く示された。

本研究により、磁性抗がん剤による高齢者に向けた安心・安全な悪性中皮腫の抗がん治療を開発することが、本申請の最大の目標であり社会貢献である。

3. 倫理面への配慮

本研究は、厚生労働省の所管する実施機関における動物実験等の実施に関する基本指針及び横浜市立大学医学部で定めた倫理規定等を遵守して行う。動物を用いた実験は、動物実験の講習を修了し、十分な知識と経験を有するものだけに従事させる。産学連携、他施設共同、臨床試験、薬事申請に当たっては、関係者および関係施設における利益相反を中心に守秘義務など各種コンプライアンスを十分に順守して行う。また生物統計においては、動物愛護の観点から、必要とされる動物数などを最小限にとどめるため、本学臨床試験センターの指導下で生物統計の専門家の指導を受けつつ行う。

4. 発表論文など

1. Okamoto Y, Hirota M, Monden Y, Murata S, Koyama C, Mitsudo K, Iwai T, Ishikawa Y, and Tohnai I: High-dose zoledronic acid narrows the periodontal space in rats. *Int J Oral Maxillofac Surg.* 42:627-631, 2013
2. Saito S, Hasegawa S, Sekita A, Bakalova R, Furukawa T, Murase K, Saga T, Aoki I: Manganese-enhanced MRI reveals early-phase radiation-induced cell alterations in vivo. *Cancer Res.* 73:3216-24, 2013.
3. Sawada K, Horiuchi-Hirose M, Saito S, Aoki I: MRI-based morphometric characterizations of sexual dimorphism of the cerebrum of ferrets (*Mustela putorius*). *Neuroimage.* 2013 *in press*
4. Ota S, Takahashi Y, Tomitaka A, Yamada T, Kami D, Watanabe M, Takemura Y: Transfection efficiency influenced by aggregation of DNA/polyethylenimine max/magnetic nanoparticle complexes *J Nanoparticle Res.* 15:1-12, 2013.
5. Song Z, Yamada T, Shitara H and Takemura Y: Quantitative Analysis of Transverse Cracking of Rail using Eddy Current Non-Destructive Testing *Appl Mechan Mat.* 249-250:70-75, 2013.
6. 神奈川新聞 平成25年11月8日 「未来医療への架け橋 がん治療 磁石の力応用試みる」
7. なお、平成25年度においては本研究関連の特許申請(PCT)を5件行った。

Prostaglandin E₂ Inhibits Elastogenesis in the Ductus Arteriosus via EP4 Signaling
Utako Yokoyama, Susumu Minamisawa, Aki Shioda, Ryo Ishiwata, Mei-Hua Jin, Munetaka Masuda, Toshihide Asou, Yukihiko Sugimoto, Hiroki Aoki, Tomoyuki Nakamura and Yoshihiro Ishikawa

Circulation. 2014;129:487-496; originally published online October 21, 2013;
doi: 10.1161/CIRCULATIONAHA.113.004726

Circulation is published by the American Heart Association, 7272 Greenville Avenue, Dallas, TX 75231
Copyright © 2013 American Heart Association, Inc. All rights reserved.
Print ISSN: 0009-7322. Online ISSN: 1524-4539

The online version of this article, along with updated information and services, is located on the
World Wide Web at:

<http://circ.ahajournals.org/content/129/4/487>

Data Supplement (unedited) at:

<http://circ.ahajournals.org/content/suppl/2013/10/21/CIRCULATIONAHA.113.004726.DC1.html>

Permissions: Requests for permissions to reproduce figures, tables, or portions of articles originally published in *Circulation* can be obtained via RightsLink, a service of the Copyright Clearance Center, not the Editorial Office. Once the online version of the published article for which permission is being requested is located, click Request Permissions in the middle column of the Web page under Services. Further information about this process is available in the Permissions and Rights Question and Answer document.

Reprints: Information about reprints can be found online at:
<http://www.lww.com/reprints>

Subscriptions: Information about subscribing to *Circulation* is online at:
<http://circ.ahajournals.org//subscriptions/>

Prostaglandin E₂ Inhibits Elastogenesis in the Ductus Arteriosus via EP4 Signaling

Utako Yokoyama, MD, PhD; Susumu Minamisawa, MD, PhD; Aki Shioda, MS; Ryo Ishiwata, MS; Mei-Hua Jin, PhD; Munetaka Masuda, MD, PhD; Toshihide Asou, MD, PhD; Yukihiko Sugimoto, PhD; Hiroki Aoki, MD, PhD; Tomoyuki Nakamura, MD, PhD; Yoshihiro Ishikawa, MD, PhD

Background—Elastic fiber formation begins in mid-gestation and increases dramatically during the last trimester in the great arteries, providing elasticity and thus preventing vascular wall structure collapse. However, the ductus arteriosus (DA), a fetal bypass artery between the aorta and pulmonary artery, exhibits lower levels of elastic fiber formation, which promotes vascular collapse and subsequent closure of the DA after birth. The molecular mechanisms for this inhibited elastogenesis in the DA, which is necessary for the establishment of adult circulation, remain largely unknown.

Methods and Results—Stimulation of the prostaglandin E₂ (PGE₂) receptor EP4 significantly inhibited elastogenesis and decreased lysyl oxidase (LOX) protein, which catalyzes elastin cross-links in DA smooth muscle cells (SMCs), but not in aortic SMCs. Aortic SMCs expressed much less EP4 than DASMCs. Adenovirus-mediated overexpression of LOX restored the EP4-mediated inhibition of elastogenesis in DASMCs. In EP4-knockout mice, electron microscopic examination showed that the DA acquired an elastic phenotype that was similar to the neighboring aorta. More importantly, human DA and aorta tissues from 7 patients showed a negative correlation between elastic fiber formation and EP4 expression, as well as between EP4 and LOX expression. The PGE₂-EP4-c-Src-phospholipase C (PLC) γ -signaling pathway most likely promoted the lysosomal degradation of LOX.

Conclusions—Our data suggest that PGE₂ signaling inhibits elastogenesis in the DA, but not in the aorta, through degrading LOX protein. Elastogenesis is spatially regulated by PGE₂-EP4 signaling in the DA. (*Circulation*. 2014;129:487-496.)

Key Words: elasticity ■ muscle, smooth ■ pediatrics ■ prostaglandins ■ signal transduction

Elastic fibers are the largest structures in the extracellular matrix. Beginning with the onset of pulsatile blood flow in the developing aorta and pulmonary artery, smooth muscle cells (SMCs) in the vessel wall produce a complex extracellular matrix that ultimately defines the mechanical properties that are critical for proper function of the neonatal and adult vascular system.¹ As such, hemodynamics and mechanical stress are considered to be the main regulators in the formation of the vascular elastic fiber system during development.²

Clinical Perspective on p 496

The ductus arteriosus (DA) and its connecting elastic arteries (ie, the descending aorta and the main pulmonary trunk) are exposed to essentially the same mechanical forces and hemodynamics. However, since 1914, it has been widely recognized in multiple species that the DA exhibits sparse elastic fibers in the middle layer compared with adjacent elastic arteries, as

well as disassembly and fragmentation of the internal elastic lamina.³⁻⁸ In the human fetal aorta, newly synthesized uncrosslinked elastin appears at 23 weeks of gestational age to be unevenly distributed on the surface of microfibrils, where it forms continuous strips of variable width.⁹ However, the DA exhibits fewer elastic fibers than the aorta.^{4,6} This decreased elastogenesis is the hallmark of the vascular remodeling of the DA in humans and a variety of other species.³⁻⁷ It has been suggested that this muscular phenotype of the DA allows it to collapse easily at birth when prostaglandin E₂ (PGE₂) is withdrawn and blood flow between the aorta and the pulmonary artery is reduced, thereby permitting immediate postnatal closure of the DA. Conversely, it is known that abnormalities of elastic fibers and elastic lamina are primarily responsible for the persistence of the DA in some human cases.^{10,11} These abnormalities likely prevent intimal cushion formation and make it difficult to collapse the arterial wall. Therefore, it is

Received July 2, 2013; accepted October 7, 2013.

From the Cardiovascular Research Institute, Yokohama City University, Yokohama, Japan (U.Y., S.M., A.S., R.I., M.-H.J., Y.I.); the Department of Life Science and Medical Bioscience, Waseda University Graduate School of Advanced Science and Engineering, Tokyo, Japan (S.M., R.I.); the Department of Cell Physiology, Jikei University School of Medicine, Tokyo, Japan (S.M.); the Department of Surgery, Yokohama City University, Yokohama, Japan (M.M.); the Department of Cardiovascular Surgery, Kanagawa Children's Medical Center, Yokohama, Japan (T.A.); the Department of Pharmaceutical Biochemistry, Kumamoto University, Kumamoto, Japan (Y.S.); Cardiovascular Research Institute, Kurume University, Kurume, Japan (H.A.); and the Department of Pharmacology, Kansai Medical University, Osaka, Japan (T.N.).

The online-only Data Supplement is available with this article at <http://circ.ahajournals.org/lookup/suppl/doi:10.1161/CIRCULATIONAHA.113.004726/-/DC1>.

Correspondence to Susumu Minamisawa, MD, PhD, Department of Cell Physiology, Jikei University School of Medicine, Tokyo 105-8461, Japan. E-mail sminamis@jikei.ac.jp

© 2013 American Heart Association, Inc.

Circulation is available at <http://circ.ahajournals.org>

DOI: 10.1161/CIRCULATIONAHA.113.004726

important to understand the molecular mechanisms of how elastogenesis is regulated in the DA. Although Hinek et al^{12,13} have demonstrated that truncated 52-kDa tropoelastin and the reduction of elastin binding protein negatively regulates elastic fiber formation in the DA, the mechanisms for impaired elastogenesis in the DA wall are not yet fully understood, despite nearly a century of research.⁸

During mid- to late gestation, fetuses are exposed to abundant PGE₂ that is released from the placenta¹⁴ in accordance with the time course of impaired elastic fiber formation in the DA. The biological effects of PGE₂ depend on the prostanoid EP receptor subtypes EP1 through EP4¹⁵. Among the EP subtypes, EP4 is highly expressed in the DA of multiple species, including mice, rats, and humans, and regulates the DA muscular tone.^{16–19} In addition to the DA muscular contraction, remodeling of the extracellular matrix during the fetal and neonatal period is necessary to complete the anatomical closure of the DA.^{16,20,21} Our previous studies have demonstrated the role of PGE₂-EP4 signaling in DA remodeling, in which EP4 stimulation promotes intimal thickening, which is characteristic of the remodeling of the DA, in a hyaluronan-dependent and -independent manner.^{16,21–23}

In this context, we hypothesized that PGE₂ inhibits elastogenesis in the DA through PGE₂-EP4 signaling. In the present study, we examined the molecular mechanisms of the inhibitory regulation of elastogenesis in human DA tissues and rodent DASMCs. We demonstrated that activation of EP4 promoted degradation of the mature lysyl oxidase (LOX) protein, a cross-linking enzyme for elastic fibers, only in the DA (and not in the aorta), leading to poor elastogenesis.

Methods

Expanded methods are described in the online-only Data Supplement.

Animals and Tissues

We used Wistar rat fetuses from timed-pregnant mothers (SLC Inc., Hamamatsu, Japan). Pooled tissues of the DA, aorta, and pulmonary arteries were obtained from rats on day 21 of gestation (n>60). Generation and phenotypes of EP4-knockout mice have been described previously.¹⁷ All mice were C57BL/6 background littermates from heterozygote crosses. All animal studies were approved by the institutional animal care and use committees of Yokohama City University and Waseda University.

Human Tissues of the DA

Human DA tissues were obtained from Yokohama City University Hospital and Kanagawa Children's Medical Center at the time of corrective operations. Detailed patient information is summarized in Table I in the online-only Data Supplement. The study was approved by the human subject committees at both Yokohama City University and Kanagawa Children's Medical Center. All samples were obtained after receiving written informed parental consent.

Tissue Staining and Immunohistochemistry

Elastic fiber formation was evaluated by Elastica van Gieson staining. Immunohistochemical analysis was performed as previously described.¹⁶ A color extraction method using BIOREVO bz-9000 and associated software (KEYENCE, Osaka, Japan) was performed to quantify elastic fiber formation and expression of EP4 and LOX. Three serial paraffin-embedded sections per each patient were subjected to elastica staining and immunohistochemistry. More than 19 fields in the smooth muscle layer of the DA and aorta were examined

in each slide. The area stained dark purple indicated elastic fibers and diaminobenzidine (DAB)-stained colors, EP4- or LOX-positive areas, were extracted from matched area and counted using the software. Correlations of elastic fiber formation and EP4 and LOX expression were examined using >19 independent fields within 1 patient. We examined sections from a total of 7 patients, and the correlation coefficient and *P* value of each patient are shown in Table II in the online-only Data Supplement.

Immunocytochemistry

Vascular SMCs were plated on glass coverslips in 10% FBS in DMEM. The culture medium was then changed to 10% FBS in DMEM/F-12 alone, PGE₂, AE1-329, sulprostone, butaprost, or β-aminopropionitrile fumarate (day 1). Each drug was added on day 4. To examine the effect of silencing EP4 on elastic fiber formation, reverse transfection of DASMCs with EP4-targeted siRNA was performed according to the manufacturer's instructions on days 1 and 4, and treated with AE1-329 on days 2 and 5. To examine the effect of overexpression of LOX or EP4, the cells were infected with adenoviruses at 10 multiplicities of infection on days 1 and 4. AE1-329 was added to the cells on days 2 and 5. All cells were fixed in 10% buffered formalin on day 7. The fixed cells were stained with anti-elastin antibody as previously described.²² All images were taken using a Nikon TE2000 (Nikon Instruments Inc, Tokyo, Japan) and processed under the same settings.

Quantitative Measurement of Insoluble Elastin

Newly synthesized insoluble elastin was measured as previously described.²⁴ Briefly, DASMCs were subconfluent plated on 60-mm dishes. Three days after plating, 20 μCi [³H]valine was added to each dish (day 0). AE1-329 (1 μmol/L) or phosphate-buffered saline was added on days 0 and 4. The cells were harvested in 0.1 mol/L acetic acid on ice on day 7. The cells were boiled in 0.1N NaOH for 1 h. The insoluble pellets were boiled with 5.7N HCl for 1 h. The radioactivity was measured with a scintillation counter.

Statistical Analysis

Data are shown as the mean±SEM of independent experiments. The Mann-Whitney *U* test, Kruskal-Wallis test, and Pearson correlation coefficient were used to determine the statistical significance of the data. A value of *P*<0.05 was considered significant.

Results

EP4 Signaling Inhibits Elastogenesis in the DA In Vivo

In the late gestation period, the DA exhibits disassembly and fragmentation of the internal elastic lamina and sparse elastic fibers in the middle layer compared to its two connecting arteries, the aorta and the pulmonary artery (Figure 1A), despite the fact that they are exposed to essentially the same hemodynamics. The expression of rat EP4 is greater in the DA than in the aorta and the pulmonary artery on the 21st day of gestation (day 21; Figure 1B).¹⁶ We examined the association between the expression of EP4 mRNA and elastogenesis in developing mouse fetuses (Figure 1C). In day 12.5 mice, organized elastic fibers were not observed in either the DA or the aorta, whereas *in situ* hybridization analysis revealed that the expression of EP4 mRNA was clearly higher in the DA than in the aorta or the pulmonary artery. In day 16.5 and day 18.5 mice, the formation of elastic fibers was observed more clearly in the aorta than in the DA. In these developing stages, obvious abundant expression of EP4 mRNA was observed in the DA, but not in the aorta. To examine the effect of EP4

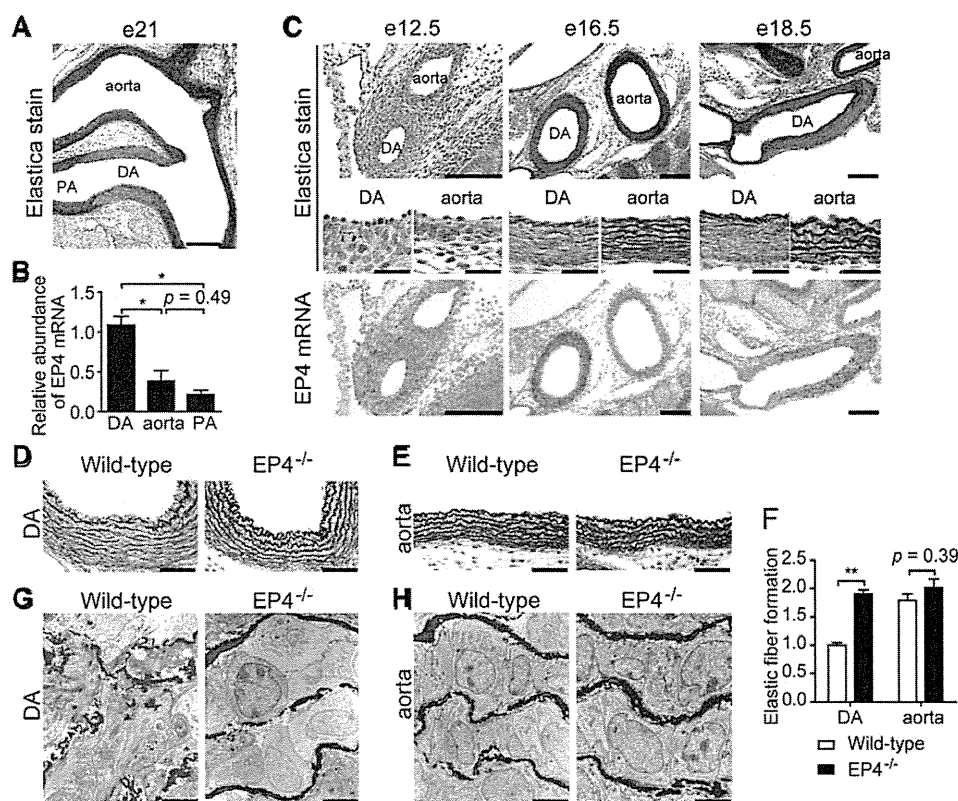


Figure 1. EP4 signaling attenuated elastic fiber formation in vivo. **A**, Elastica van Gieson stain (elastica stain) of rat fetus on day 21 of gestation (e21). **B**, Expression of EP4 mRNA of the rat ductus arteriosus (DA), aorta, and pulmonary artery (PA) on day 21 of gestation. $n=6$. **C**, Developmental changes in elastic fiber formation and EP4 mRNA by in situ hybridization in mouse fetus on days 12.5 (e12.5), 16.5 (e16.5), and 18.5 (e18.5) of gestation. Expression of EP4 mRNA was higher in the DA than in the aorta and pulmonary artery. Conversely, elastic fiber formation is sparser in the DA than in the other arteries. **D**, **E**, **G**, and **H**, Elastica stain and electron microscopic images of wild-type and EP4^{-/-} mice on day 18.5 of gestation. Elastic fiber formation was restored in the DA of EP4^{-/-} mice. **F**, Quantification of the elastic fiber formation of **D** and **E** using a color extraction method. $n=8$. * $P<0.05$, ** $P<0.01$. Scale bars, 200 μm (**A**); 100 μm (**C**, **upper** and **lower**); 50 μm (**D**, **E**); 20 μm (**C**, **middle**); 5 μm (**G**, **H**).

on elastogenesis in vivo, we examined elastic fiber formation in the DA of EP4^{-/-} mice. In EP4^{-/-} mice, which die postnatally as a result of persistent patent DA (PDA),^{17,25} we found that the DA acquired an elastic phenotype that was similar to that of the neighboring aorta, as determined by elastica staining (Figure 1D and 1E), a color extraction method of elastica staining (Figure 1F), and electron microscopic examination (Figure 1G and 1H).

Human Vascular Tissues Show a Negative Correlation Between Elastic Fibers and EP4 Expression

We also investigated the relationship between elastic fiber formation and EP4 expression in surgical samples from 7 patients with coarctation of the aorta who underwent surgical repair of aortic narrowing (Figure 2A, Table I in the online-only Data Supplement). In concurrence with the findings in rodents, there was less elastic fiber formation in the DA than in the normal aorta, and the cells stained with anti-EP4 antibody were far more abundant in the DA (Figure 2B). Indeed, statistical analysis revealed that the correlation was significant between the amount of EP4 expression and the degree of inhibited elastic fiber formation (Figure 2C, Table II in the online-only Data Supplement). Thus, elastogenesis is inhibited when EP4 is abundant. Taken together, these in vivo data

suggest that EP4 plays a primary role in the inhibition of elastogenesis of the DA in humans and rodents.

EP4 Signaling Inhibits Elastogenesis in DAsMCs

To clarify the role of EP4 in elastogenesis in detail, we evaluated the elastic fiber assemblies in rat DAsMCs using an in vitro system, as reported previously.²⁴ In the control group, DAsMCs developed an abundant meshwork of elastic fibers (Figure 3A). In the presence of PGE₂ or the EP4 agonist ONO-AE1-329, however, DAsMCs developed a poor meshwork of elastic fibers. Neither the EP1/3 agonist sulprostone nor the EP2 agonist butaprost had any effect on elastic fiber development. LOX is a cross-linking enzyme that forms insoluble mature elastic fibers. Its specific small molecule inhibitor β -aminopropionitrile fumarate impaired elastic fiber formation (Figure 3A). To quantify the amount of mature (ie, cross-linked) elastic fibers inhibited by EP4 stimulation, we metabolically labeled newly synthesized elastin with [³H] valine, and measured the incorporation of [³H]valine in the NaOH-insoluble fraction of these cells, which reflects the amount of newly synthesized mature elastic fibers.²⁴ As shown in Figure 3B, in DAsMCs, we detected a significant decrease in the incorporation of [³H]-valine into the insoluble fraction when ONO-AE1-329 was added to the medium (Figure 3B). When the expression of EP4 mRNA was decreased by 89%

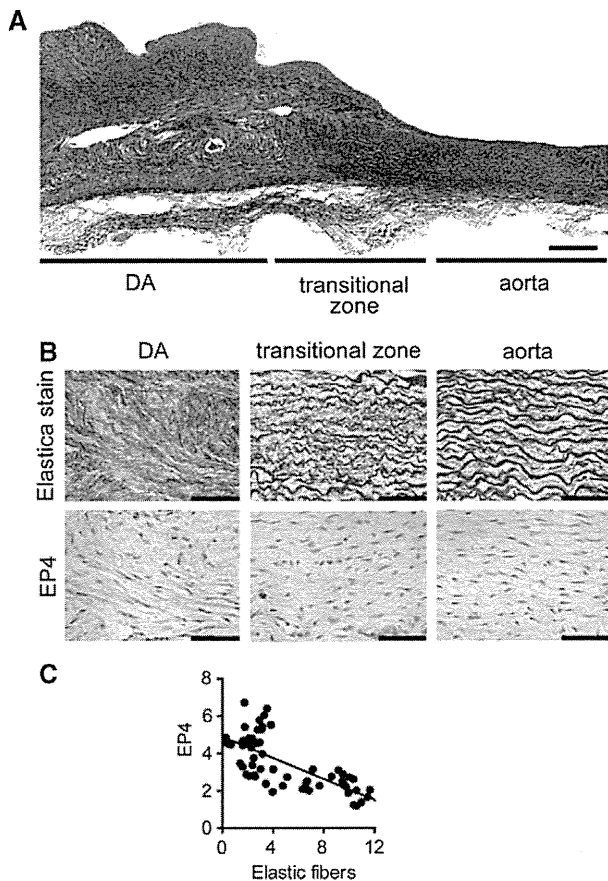


Figure 2. Human vascular tissues show a negative correlation between elastic fibers and EP4 expression. **A**, A representative image of the elastica stain of a human neonatal vessel. **B**, Elastica stain and immunohistochemistry for EP4 in human neonatal vessels. **C**, Representative results of quantification of elastic fiber formation and EP4 protein expression using a color extraction method. Values are shown in arbitrary units. Scale bars, 200 μm (**A**); 50 μm (**B**).

by RNA interference, DASCs developed elastic fiber formation even in the presence of ONO-AE1-329 (Figure 3C). To further confirm the existence of EP4-mediated impaired elastic fiber formation, we used rat aortic SMCs, which express much less EP4 than DASCs (Figure 3D). When EP4 was forcibly expressed in aortic SMCs by EP4 gene transfer, elastogenesis was markedly impaired by ONO-AE1-329, whereas ONO-AE1-329 did not attenuate elastic fiber formation in the LacZ control (Figure 3E). These *in vitro* results indicate that PGE_2 -EP4 stimulation is responsible for the impaired elastogenesis of the DA.

EP4 Signaling Inhibits Elastic Fiber Formation by Decreasing LOX Protein

In the process of elastic fiber assembly, soluble elastin precursors (tropoelastin) are deposited on microfibrils.^{1,26} They are then cross-linked by LOX, which confers elastic properties to elastic fibers.²⁷ Inactivation of the *LOX* gene is known to cause structural alterations in the arterial walls, leading to cardiovascular abnormalities.²⁸ In this context, we investigated the expression of LOX protein in human surgical samples. In contrast to EP4, there were significantly fewer cells stained with

anti-LOX antibody in the DA (Figure 4A). When elastic fiber formation and the expression of EP4 and LOX were quantified, LOX expression was positively correlated with elastic fiber formation, whereas it was negatively correlated with EP4 expression (Figure 4B, Table II in the online-only Data Supplement). Interestingly, elastic fiber formation and EP4- or LOX-positive cells in the transitional zone appeared intermediate between the DA and aorta. We think that this finding supports previous reports that suggested that the coarctate ridge, a narrowed pathological segment in the aorta, is formed by mixed tissues from the native aorta and migrated tissues of DA origin.^{29,30}

Next, we examined the effect of EP4 stimulation on LOX protein expression. We found that the amount of mature LOX form was significantly decreased in the culture media of DASCs and DASC lysates in the presence of PGE_2 and ONO-AE1-329 (Figure 4C and 4D). The effects of ONO-AE1-329 were dose- and time-dependent (Figure 4E and 4F). Other EP isoform-specific agonists had little effect. Interestingly, stimulation of EP4 did not change the expression levels of tropoelastin and fibrillin-1 proteins, which are the main components of elastic fibers (Figure IA–ID in the online-only Data Supplement). In the next LOX detection, we used whole cell lysate containing both intracellular and extracellular LOX protein. Although these EP4-mediated effects were not detected in aortic SMCs (ASMCs), the EP4 agonist significantly decreased the expression of LOX protein in ASMCs when EP4 expression was induced using the adenovirus (Figure 4G and 4H). When LOX expression was induced using the adenovirus (Figure IIA and IIB in the online-only Data Supplement), elastogenesis was largely restored in the ONO-AE1-329–treated DASCs (Figure 4I). Thus, the reduction in LOX played a primary role in the EP4-mediated impairment of elastogenesis. The expression levels of matrix metalloproteinases and their activity were not altered in the DASCs by EP4 stimulation (Figure IIIA and IIIB in the online-only Data Supplement). Nor was there any difference in matrix metalloproteinase 2 activity between rat tissues of the DA and aorta (Figure IIIC in the online-only Data Supplement), suggesting that EP4 signaling plays a role in inhibiting elastogenesis, but not in promoting elastolysis in the DA.

The c-Src-PLC Signal Pathway Plays a Role in the PGE_2 -EP4-Induced Reduction in LOX Protein

Next, we examined the downstream signal pathway responsible for the EP4-mediated reduction in LOX protein expression levels. Although our previous studies have demonstrated that cAMP and its downstream pathways play a primary role in EP4-mediated DA remodeling,^{16,22,23} the cAMP–protein kinase A or cAMP–exchange protein activated by the cAMP pathway did not play a role in the EP4-mediated reduction in LOX protein (Figure 5A and 5B). Instead, we found that the EP4-induced reduction in LOX protein was restored by the PLC inhibitor U73122 (Figure 5C–5E), but not by $\text{G}\beta\gamma$, protein kinase C, or phosphoinositide 3-kinase inhibitors (galein, bisindolylmaleimide I, LY294002; Figure 5C and 5D). Furthermore, the PLC activator *m*-3M3FBS significantly decreased the expression levels of LOX protein in DASCs

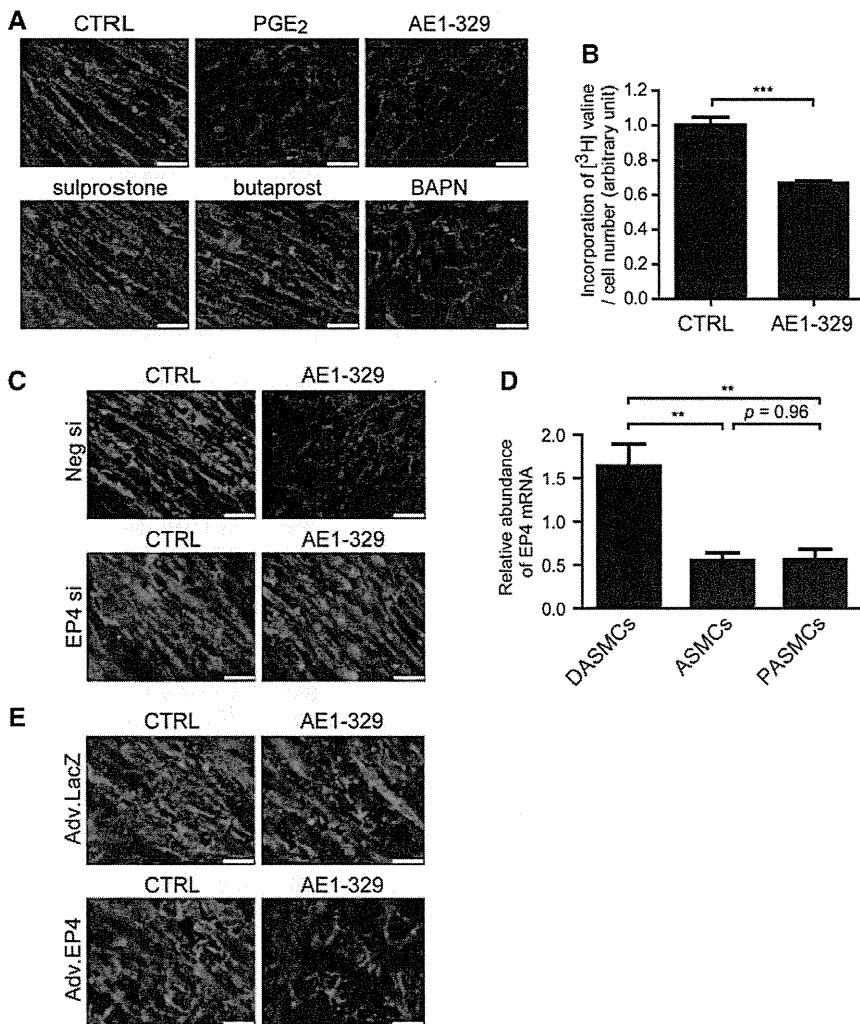


Figure 3. EP4 signaling attenuated elastic fiber formation in vitro. **A** and **C**, Immunostaining for elastin (red) and DNA (blue) of ductus arteriosus smooth muscle cells (DASMCs) treated with each drug indicated or EP4-targeted siRNA (EP4 si). AE1-329 indicates ONO-AE1-329; CTRL, control; and Neg si, negative control siRNA. Pharmacological activation of EP4 by ONO-AE1-329 attenuated elastic fiber formation. **B**, Incorporation of [³H]valine was quantified in DASMCs treated with or without AE1-329. n=8, ***P<0.001. **D**, Expression of EP4 mRNA in DASMCs, aortic SMCs (ASMCs), and pulmonary SMCs (PASMCs). n=6, **P<0.01. **E**, Immunostaining for elastin (red) and DNA (blue) of the EP4- or LacZ-overexpressing ASMCs treated with or without AE1-329. Activation of EP4 did not affect elastic fiber formation in LacZ-overexpressing ASMCs, whereas it decreased elastic fiber formation in EP4-overexpressing ASMCs. Each drug was used at 1 μmol/L. Scale bars, 20 μm.

(Figure 5F). Because several recent studies have demonstrated that PGE₂ promotes cancer cell migration via the EP4-c-Src signal pathway^{31,32} and that c-Src plays a critical role in the phosphorylation of PLCγ in several cell types,^{33,34} we hypothesized that the c-Src-PLCγ signal pathway may be involved. We found that ONO-AE1-329 significantly increased PLCγ1 phosphorylation (Figure 5G). In contrast, the Src-family kinase inhibitor PP2 significantly decreased PLCγ1 phosphorylation (Figure 5H and 5I) and restored the reduction in LOX protein induced by ONO-AE1-329 (Figure 5J and 5K). These results support our hypothesis that the c-Src-PLCγ signal pathway plays a primary role in the PGE₂-EP4-induced reduction in LOX protein.

EP4 Signaling Promotes LOX Degradation in Lysosomes

Although ONO-AE1-329 decreased the expression of LOX protein in DASMCs, we found that ONO-AE1-329 did not decrease the mRNA expression of LOX (Figure 6A). Active LOX is synthesized as a 50-kDa inactive LOX proenzyme (pro-LOX), which is secreted into the extracellular space. Pro-LOX is then processed by proteolysis into a functional 32 kDa enzyme LOX and an 18-kDa propeptide.^{27,35} Using a pro-LOX-specific antibody, we found that the pro-LOX protein

itself was not decreased by ONO-AE1-329 (Figure 6B and 6C), indicating that LOX was decreased post-translationally. BMP1 is a major protease that cleaves pro-LOX in the extracellular space.²⁷ However, ONO-AE1-329 did not change the expression of BMP1 mRNA or protein in DASMCs (Figure IVA and IVB in the online-only Data Supplement). Instead, we found that lysosomal degradation inhibitors, such as NH₄Cl and bafilomycin, eliminated the EP4-induced reduction in LOX protein (Figure 6D and 6E). These lysosomal degradation inhibitors also restored the PLC-mediated reduction in LOX protein (Figure 6F and 6G). Furthermore, we found that the clathrin-mediated endocytosis inhibitors chlorpromazine and phenylarsine oxide similarly restored the EP4-induced reduction in LOX protein (Figure 6H–6J). Administration of chlorpromazine also restored the PLC-induced reduction in LOX protein (Figure 6K and 6L). In comparison, the caveolar endocytosis inhibitor methyl-beta-cyclodextrin (MβCD), the macropinocytosis inhibitor ethylisopropylamiloride (EIPA), and the proteosomal inhibitor MG132 showed little or no effect on LOX protein reduction (Figure VA–VC in the online-only Data Supplement). These data suggest that PGE₂-EP4-PLC stimulation promotes the degradation of the LOX protein in lysosome through clathrin-mediated endocytosis.

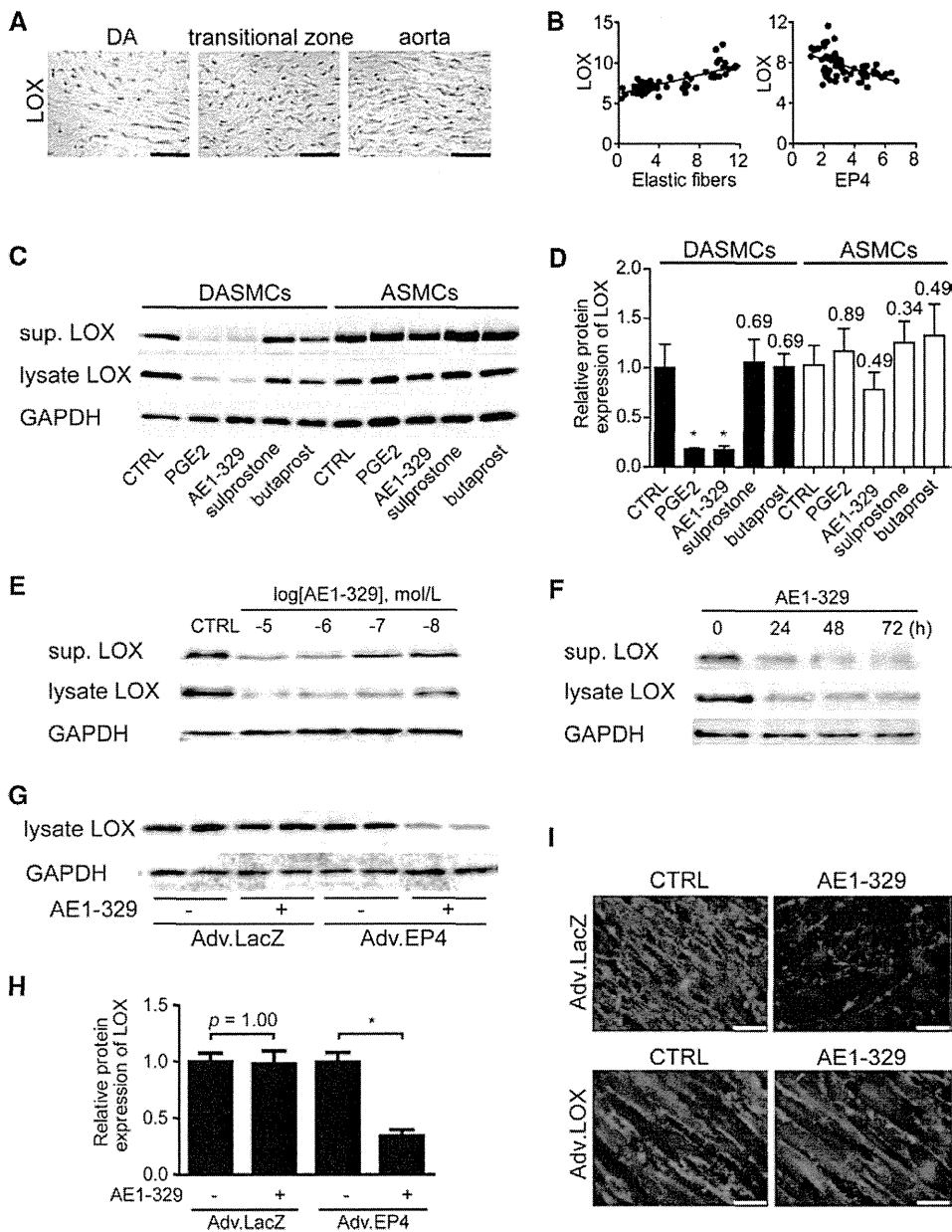


Figure 4. EP4 signaling attenuated elastic fiber formation via decreased lysyl oxidase (LOX) expression. **A**, Representative images of immunohistochemistry for LOX in human neonatal vessels. **B**, Representative results of quantification of elastic fiber formation, LOX, and EP4 protein expression using a color extraction method. Values are shown in arbitrary units. **C**, Western blotting for LOX in supernatant (sup.) and lysate of smooth muscle cells (SMCs) treated for 72 h. **D**, Quantification of **C**. n=4, *P<0.05 vs CTRL. Numbers on the bars indicate P values. Administration of prostaglandin E₂ (PGE₂) or the EP4 agonist AE1-329 decreased the mature LOX form in both supernatant and lysate of ductus arteriosus SMCs (DASMCS) but not in aortic SMCs (ASMCS). **E**, Dose-dependent effects of AE1-329 (24 h incubation) on LOX protein in DASMCS. **F**, Time-dependent reduction in LOX protein in DASMCS. **G**, Protein expression of LOX was decreased in EP4-overexpressing ASMCS (Adv. EP4) treated with AE-329 for 24 h. **H**, Quantification of **G**. n=4, *P<0.05 vs CTRL. **I**, Immunostaining for elastin (red) and DNA (blue) of the LOX- or LacZ-overexpressing DASMCS treated with or without AE1-329. Each drug was used at 1 μmol/L. Scale bars, 50 μm (**A**); 20 μm (**I**).

Discussion

Although it is widely recognized in multiple species that the DA exhibits sparse elastic fibers in the middle layer and disassembly and fragmentation of the internal elastic lamina, the molecular mechanism for these has not yet been identified. The current study demonstrated a novel role of PGE₂ in spatially regulating elastogenesis by LOX protein degradation via the EP4-c-Src-PLCγ signal pathway in the DA, which contributes to the transition from fetal to neonatal circulation. Previous studies have demonstrated that abnormalities of elastic fibers are primarily responsible for PDA in some human cases.^{10,11} According to the Gittenberger-de Groot group's¹⁰ observation, there are several types of abnormal elastogenesis that can cause PDA. The following 2 types are of particular importance: (1) thickened subendothelial elastic lamina with sparse or slightly increased elastic fibers in the media, and (2) aortification of the ductal wall. PDA with aortification of the

ductal wall in EP4-knockout mice resembles the latter phenotype. These abnormalities of elastic fibers are likely to prohibit intimal cushion formation and make it difficult to collapse the arterial wall. This suggests that the control of elastogenesis is clinically important. Pharmacological treatment for PDA, such as indomethacin after birth, may have an adverse effect on the inhibition of elastic fiber formation in the DA, especially in premature infants. This should be further investigated in a future study.

The EP4 receptor is highly expressed in the DA compared to the adjacent arteries¹⁶; it is coupled to G_{αs} and increases intracellular cAMP formation. The roles of EP4-cAMP signaling have been well studied in the DA. We and others have demonstrated that EP4 signaling induces vasodilation and hyaluronan-mediated vascular remodeling of the DA through cAMP-dependent protein kinase A^{16,21,23} and that it promotes the migration of DASMCS and subsequent intimal thickening